BMC Medical Genomics

RESEARCH

Open Access

New insight into the development of synpolydactyly caused by expansion of HOXD13 polyalanine based on weighted gene co-expression network analysis

Xiumin Chen[1], Xiaofang Shen[2], Tao Yang[1], Yixuan Cao[1] and Xiuli Zhao[1*]

Abstract

Background Synpolydactyly (SPD) is mainly caused by mutations of polyalanine expansion (PAE) in the transcription factor gene *HOXD13* and the involved cell types and signal pathway are still not clear possible pathways and single-cell expression characteristics of limb bud in *HOXD13* PAE mice was analyzed in this study.

Method We investigated a previous study of a mouse model with SPD and conducted weighted gene co-expression network analysis (WGCNA) using a single-cell RNA sequencing dataset from limb bud cells of SPD mouse model of *HOXD13* + 7A heterozygote.

Results Analysis of WGCNA revealed that synpolydactyly-associated *Hoxd13* PAEs alter the immune response and osteoclast differentiation, and enhance DNA replication. *Bmp4*, *Hand2*, *Hoxd12*, *Lnp*, *Prrx1*, *Gmnn*, and *Cdc6* were found to play potentially key roles in synpolydactyly.

Conclusions These findings evaluated the main genes related to SPD with PAE mutations in *HOXD13* and advance our understanding of human limb development.

Keywords *Synpolydactyly*, *HOXD13*, Polyalanine expansion, Single-cell RNA sequencing, Immune response

Backgound

Synpolydactyly (SPD; MIM 186000), also known as syndactyly type II, is a distal limb deformity characterized by fusion of the third and fourth fingers, the fourth and fifth toes, and the presence of extra fingers in the syndactylous web [1]. Synpolydactyly is caused by mutations in transcription factor gene *HOXD13*. Such mutations include polyalanine expansion (PAE), point mutations and a 14 bp small deletions, and majority of SPD patients result from an incomplete trinucleotide repeat expansion within the polyalanine coding region in the first exon of the *HOXD13* gene. However, the involved cell types and signaling pathways remain unclear. Correlation between the severity of SPD and the PAE length of *HOXD13* has been discussed for many years [2]. The expansion of two alanines does not have pathological consequences [3], and, to our knowledge, PAE of less than seven alanines has not been reported in SPD patients. This means that synpolydactyly can be caused only when polyalanine expansion reaches a certain threshold, such as a PAE of seven alanines or more [4].

*Correspondence:
Xiuli Zhao
xiulizhao@ibms.pumc.edu.cn
[1] McKusick-Zhang Center for Genetic Medicine, State Key Laboratory for Complex Severe and Rare Diseases, Institute of Basic Medical Sciences Chinese Academy of Medical Sciences, School of Basic Medicine, Peking Union Medical College, Beijing 100005, China
[2] Pediatric Orthopedics, Children's Hospital of Soochow University, Suzhou, China

A recent study suggested that a novel missense mutation of *Hoxd13* (NM_000523: exon2: c.G917T: p.R306L) promoted osteoclast differentiation by regulating the Smad5/p65/c-Fos/Rank axis, which might provide a new insight into SPD development [5]. Few prior studies focused on osteoclasts. A triple of *HOXD10*, *HOXD11,* and *HOXD13* knockdown significantly decreased the number of $TRAP^{+}$-stained osteoclasts within tumor tissue while their number in bones was not affected [6]. The effect of SPD related *HOXD13* mutation on osteoclasts may be a parallel regulatory process of multi-gene changes.

Although we found that PAE of *HOXD13* affected limb development, it was unclear which cells co-expressed common transcription factors or coordinated regulation by independent transcription factors with similar activation patterns during this process. Thus, in this study we performed bioinformatics analysis using a single-cell RNA sequencing (scRNA-seq) dataset of limb bud cells from a previous study in order to analyze PAE-associated cell type–specific gene expression changes in wild-type (WT) and + 7A repeat-expanded HOXD13 allele (spdh) mice [7].

Methods

Database retrieval

Based on a retrieval of polyalanine-expanded HOXD13 allele related databases, a single-cell RNA sequencing (scRNA-seq) dataset of limb bud cells from a previous study were obtained from GSE128818. Advanced analysis was performed in these data.

Single-cell analysis

Single-cell analysis was used to assess and validate the expression level of hub genes. Quality control, dimensional reduction, and clustering of the scRNA-seq data of the mouse limb (GSE128818) were performed using Seurat (v3.1.0). After obtaining a gene expression matrix generated by Cell Ranger software [8], based on the filtered cell–gene expression matrix, we used Seurat to standardize the data and perform cell typing through reduction and clustering and to then identify characteristic genes of the different cell populations. Genes with equal or above two-fold change in relative expression levels between the mutant group and wildtype group, along with an FDR-adjusted p value < 0.05 were considered differentially expressed. Further details are listed in Supporting information Data S2.

Weighted gene co-expression network analysis

Weighted gene co-expression network analysis (WGCNA) is a systematic biological method that describes the pattern of gene associations between different samples. It can be used to identify highly synergistically altered gene sets as well as candidate biomarker genes or therapeutic targets based on the associations of gene sets, and associations between gene sets and phenotype. WGCNA was performed using a WGCNA package in R [9] to classify genes into modules. The analysis prevealed modules, or groups of related genes, which can reflect either shared regulation by common transcription factors or coordinated regulation by independent transcription factors with similar patterns of activation. Specifically, these groups were determined based on the scRNA-seq data of E12.5 limb buds from wild type (WT) and spdh mice. The selection of a β value for establishing an adjacent matrix makes our gene distribution conform to a scale-free network according to the degree of connectivity: the soft threshold (power) represents the weight, and the ordinate represents the correlation between the connectivity k and p (k). It is generally required that the correlation between k and p (k) reaches 0.85 as the value of β. Modules with a correlation coefficient greater than 0.8 (i.e., the coefficient of dissimilarity is less than 0.2) are combined [9]. Gene expression modules and different cell-type relationships are presented between spdh and WT small conditional (sc)RNA-sequence (seq) data. The eigenvector gene of each module is calculated as the first principal component gene E of a particular module and represents the overall level of gene expression within the module. We then calculated Student asymptotic P values for these correlations and corrected for the effects of multiple tests using the false discovery rate (FDR) [10]. Modules of highly coexpressed genes with |correlation coefficients| > 0.6 and an FDR < 0.05 were considered cell-type–related modules, and genes in these modules were considered cell-type–associated genes. Finally, the module eigengene was calculated and the Pearson correlation analysis was performed; hub modules and cell cluster were thus identified.

To evaluate the function of putative genes, gene ontology (GO) enrichment analysis was performed using the R package ClusterProfiler [11]. Kyoto Encyclopedia of Genes and Genomes (KEGG) enrichment analysis was performed using g: Profiler [12]. To determine the biological processes and involved signaling pathways. FDR < 0.05 was set up to identify the statistically significant enrichments in the gene clusters of the modules. Significance was assessed using Fisher's exact test.

Statistical analysis

The R software (version: 4.0.5) was used to perform all statistical analyses and graphical representations. For continuous variables, Student's t-tests were used to compare two distinct groups. For categorical variables, chi-square tests were performed.

Results

Gene modules derived from WGCNA based on gene expression of a scRNA-seq dataset of limb bud cells

To define the cell types, we annotated each cell type based on the expression levels of canonical cell-type–specific markers according to a previous study [7]. In total, we identified 16 cell states (erythrocytes, perichondrium, proximal chondrocytes, proliferating cells, interdigital mesenchymal cells, myoblasts, hematopoietic cells) using Seurat analysis. The expression levels of specific marker genes for each cell type are shown in dot plots (Fig. 1A). The top four differentially expressed genes (DEGs; sorted by adjusted *p* value, with an adjusted *p* value of < 0.05) in each cell type are shown (Fig. 1B).

Based on the characteristics of different genes in the limb bud, we used WGCNA to construct a co-expression network to identify modules and genes that were significantly related to cell-type–specific gene expression and *HOXD13* PAE. The scale-free topologies of the networks were assessed for various β shrinkage parameter values according to the WGCNA user manual, wherein a β = 5 value provided a satisfactory fit to scale-free topology. Both the adjacent matrix and topological matrix were obtained according to the β value and whether the storage network under the selected β value approximated the scale-free topology (Fig. 2A). A topologically overlapping heat map of 1227 highly variable gene pairings was selected from scRNA-seq data. The genes were clustered using dissimilarity between them, and then the tree was cut into different modules using dynamic shearing: seven modules for spdh and WT limbs (Fig. 2B and C). Both rows and columns represent a single gene, with dark, turquoise, yellow, and blue modules indicating a high degree of topological overlap (Fig. 2D). Myoblasts had the most significant correlation with the turquoise module (correlation coefficient = 0.83, Fig. 2E). Interestingly, we found that the proportion of differentially expressed genes in both significant (correlation coefficients > 0.6) and other modules was not significantly different (Fig. 2F), suggesting that the different single-cell types do not exhibit expression changes. The proportion of differentially expressed genes in the blue module, which included *Hoxd13*, was also not significantly different from that of

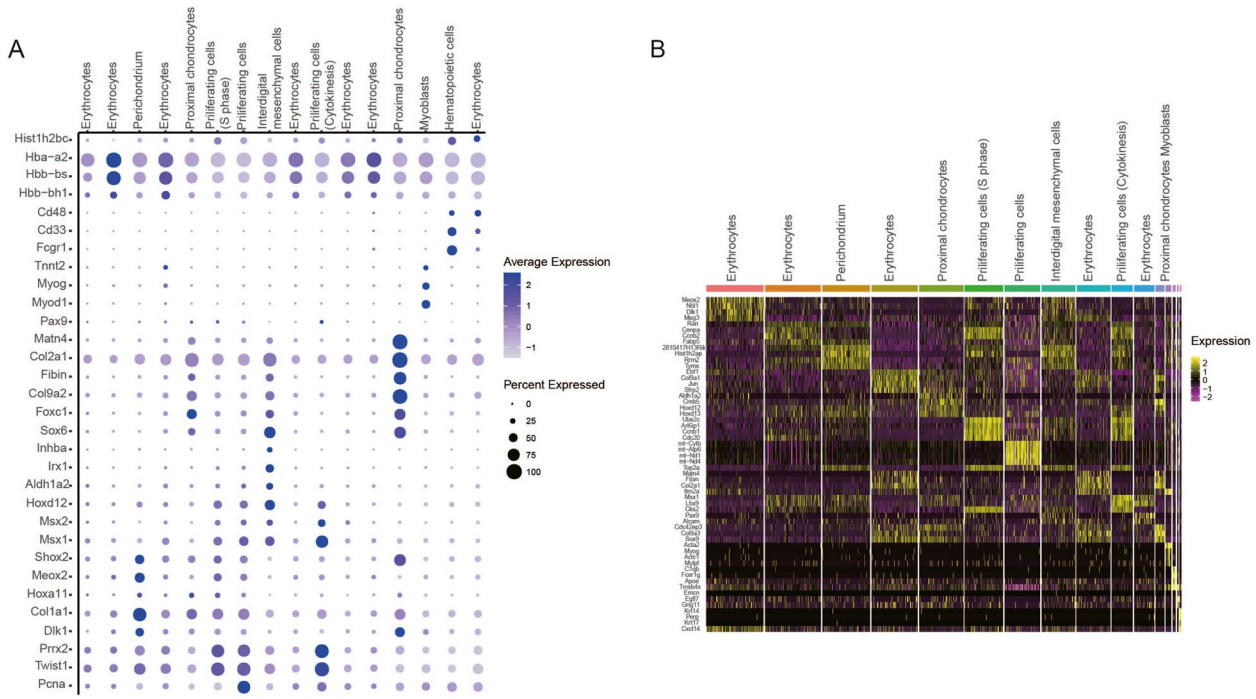

Fig. 1 The expression levels of specific marker genes were labeled for each cell type using Seurat analysis. **A** Dot plots showing the expression levels of specific marker genes for each cell type using Seurat analysis. **B** Heatmap showing the top four differentially expressed genes (DEGs) (sorted by adjusted *p* value, with an adjusted *p* value of < 0.05) (column) in each cell type (row). The color key from purple to yellow indicates gene expression levels from low to high

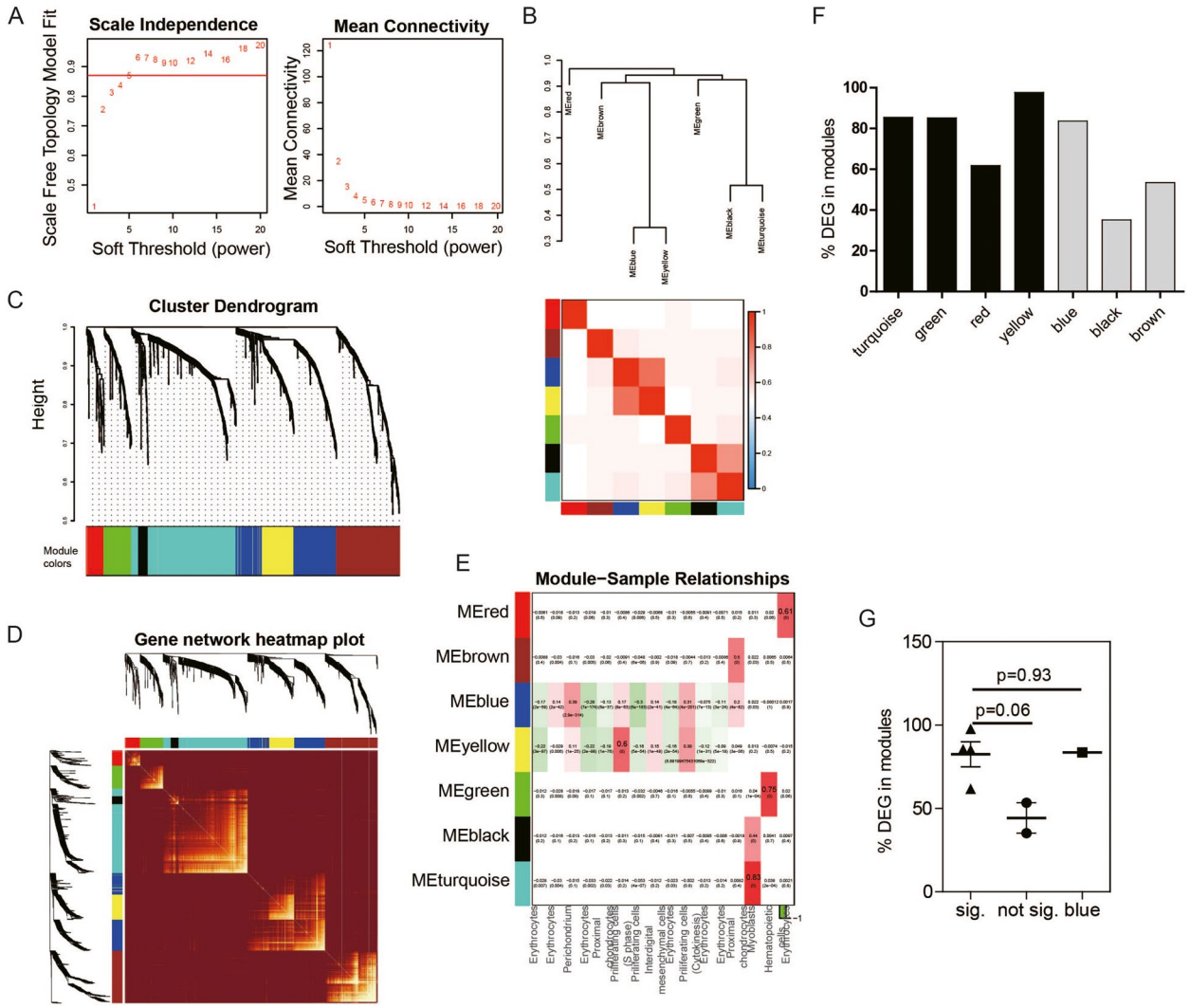

Fig. 2 Weighted correlation network analysis of the scRNA-seq data. **A** Plot of scale-free topology and mean connectivity with regards to soft-thresholding power for samples from scRNA-seq data. Red line indicates an R^2 cut-off of 0.87. **B** Visualization of the eigengene network representing the relationships among the modules and the topology of genes. **C** Clustering dendrogram showing correlations between modules from scRNA-seq data. **D** A gene co-expression network of single cells from the limb bud was constructed by weighted correlation network analysis. The hierarchical clustering and module assignment of genes are shown along the left side and top. **E** Gene expression modules showing correlations in relation to cell type. Positive correlations are red while negative correlations are green. The module and the sample traits are related to the heat map, the row represents the module, and the column represents the trait. The values in the box indicate correlation and FDR. **F** Relative numbers of DEGs identified in each module. Black bars represent |correlation coefficients|> 0.6 and FDR < 0.05 modules, and gray bars represent all other modules. G The box plot shows the relative number of DEGs in significant (sig.) modules and not significant (not sig.) modules compared with the blue module (including *Hoxd13*)

other modules (Fig. 2G), suggesting that genes in the blue module may not be involved in SPD.

Synpolydactyly-associated polyalanine expansions alter the immune response and differentiation

The gene significance across modules for myoblasts from spdh and WT scRNA-seq data was most significant for the turquoise module (Fig. 3A). The correlation coefficient between the turquoise module and the gene significance for myoblasts from spdh and WT scRNA-seq data was 0.97 ($p < 1e\text{-}200$, Fig. 3B). The top four differentially expressed genes of myoblasts in each module in spdh and WT scRNA-seq data were *Tmsb4x*, *Fcer1g*, *C1qb*, and *Apoe* (Fig. 3C).

Examination of common transcription factors or coordinated regulation by independent transcription factors with similar patterns of activation within the turquoise module revealed immune response changes

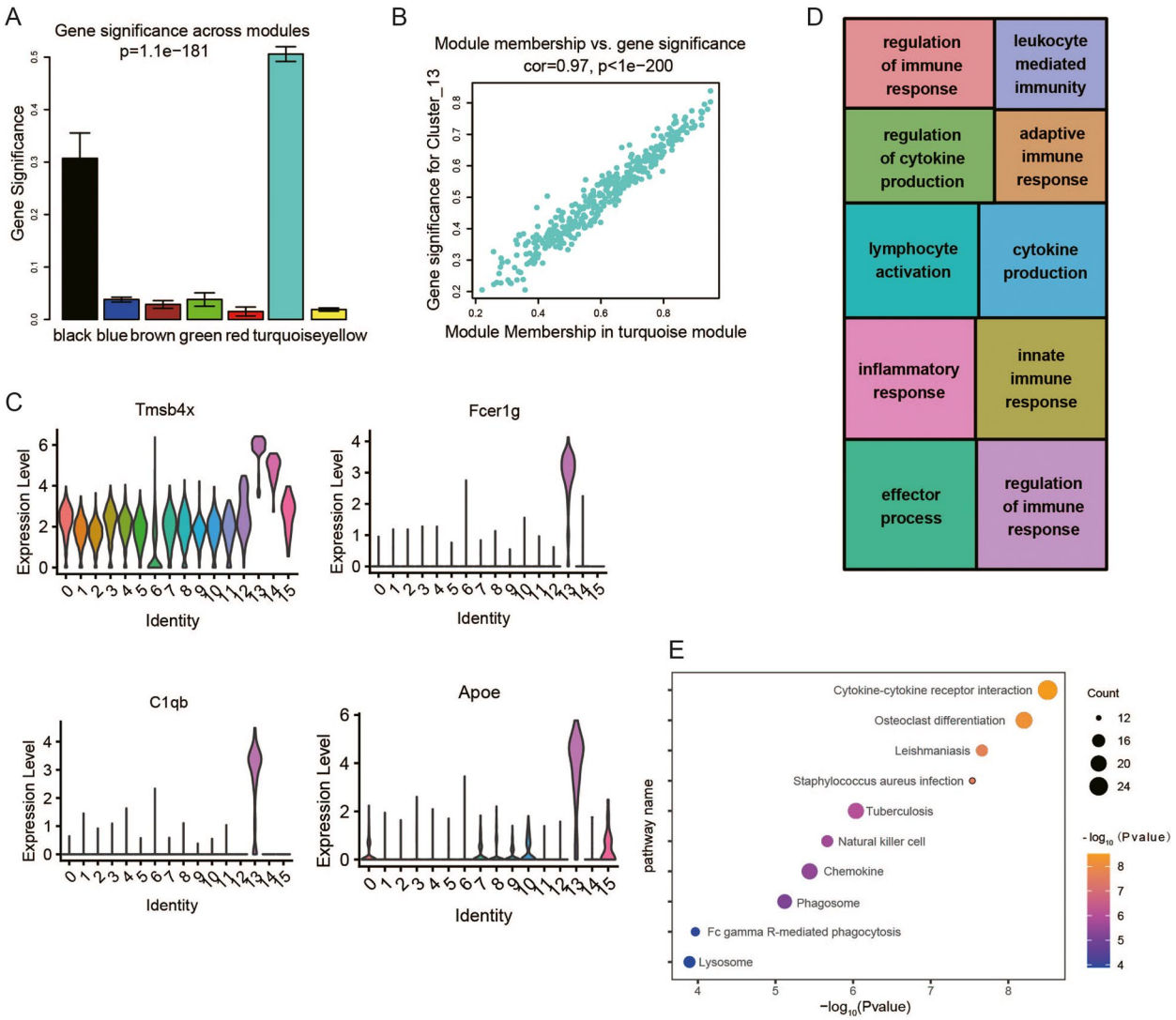

Fig. 3 Synpolydactyly-associated polyalanine expansions alter the immune response and osteoclast differentiation. **A** Gene significance across modules for myoblasts from spdh and WT scRNA-seq data. **B** Module membership in the turquoise module and gene significance for myoblasts from spdh and WT scRNA-seq data. **C** Expression of four differential genes of myoblasts in each module from spdh and WT scRNA-seq data. **D** Treemap of the top 10 condensed gene ontology (GO) terms for the turquoise module from spdh and WT scRNA-seq data, with box size corresponding to the number of significant terms associated with the GO category. **E** Representative KEGG pathways of the turquoise module from spdh and WT scRNA-seq data. "Count" stands for gene number. The color keys from yellow to blue indicate the range of the *p* value

in spdh and WT limbs, such as the immune effector process, inflammatory response, and innate immune response (Fig. 3D, Supplementary Data S1).

Moreover, to further assess turquoise module–related signaling pathways, we performed KEGG enrichment analysis. As shown in Fig. 3E, the turquoise module was mainly enriched in cytokine–cytokine receptor interaction, osteoclast differentiation, leishmaniasis, *Staphylococcus aureus* infection, tuberculosis, natural killer cell–mediated cytotoxicity, chemokine signaling pathway, phagosome, Fc gamma R–mediated phagocytosis, and lysosome (Supplementary Data S1).

Synpolydactyly-associated polyalanine expansions alter DNA replication

The top four differential genes of proximal chondrocytes in each module in spdh and WT scRNA-seq data were *Hoxd13*, *Hoxd12*, *Aldh1a2*, and *Creb5* (Fig. 4A). The gene significance across modules for proximal chondrocytes from spdh and WT scRNA-seq data showed that

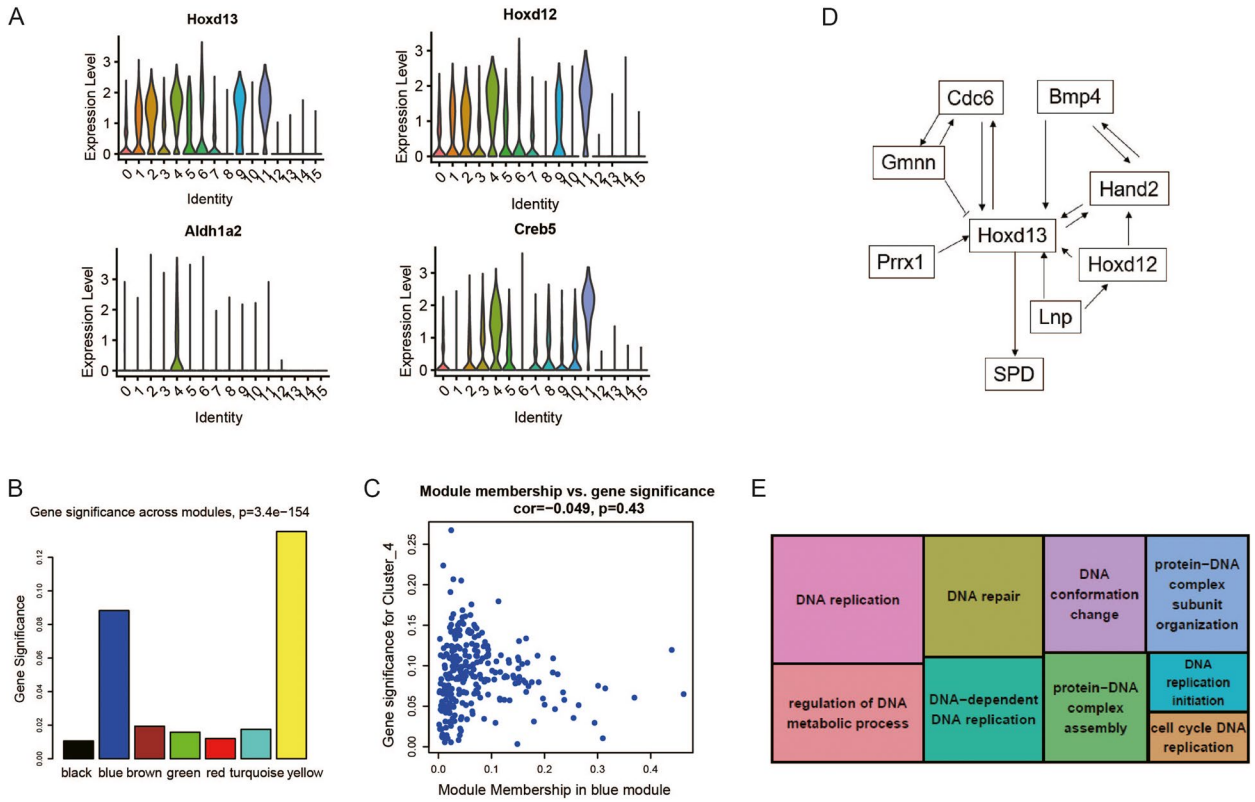

Fig. 4 Synpolydactyly-associated polyalanine expansions alter the DNA replication. Comparing the scRNA-Seq data from the limb buds of spdh and WT indicated: **A** Expression of four differential genes of proximal chondrocytes in each cell type. **B** Module membership in the blue module and gene significance for proximal chondrocytes. **C** Gene significance across modules for proximal chondrocytes related to *Hoxd13*. **D** Protein–protein interaction network of the blue module and the schematics how might Hoxd13 and its partners might be involved in SPD phenotype. **E** Treemap of the top 10 condensed gene ontology (GO) terms, with box size corresponding to the number of significant terms associated with the GO category

the blue module, which included *Hoxd13*, was the most significant module (Fig. 4B). The correlation coefficient between the blue module and the gene significance for proximal chondrocytes from spdh and WT scRNA-seq data was −0.049 ($p=0.43$, Fig. 4C).

We used STRING [13] to obtain protein–protein interactions. *Bmp4*, *Hand2*, *Hoxd12*, *Lnp*, *Prrx1*, *Gmnn*, and *Cdc6* were identified as hub genes (Fig. 4D). Examination of common transcription factors or coordinated regulation by independent transcription factors with similar patterns of activation within the blue module revealed DNA replication changes between the limb buds of spdh and WT, such as regulation of DNA metabolic process, DNA repair, DNA conformation change, and DNA-dependent DNA replication (Fig. 4E).

Discussion

Synpolydactyly (SPD) is an autosomal dominant disease caused by mutations in *HOXD13* gene. Although the genetic etiology of SPD is well known, but the detail functional mechanism of HOXD13 mutations remains unknown. Point mutations, frameshift mutations, or PAE mutations in *HOXD13* can lead to the typical SPD phenotype [14]. Some findings highlight the value of long-read whole genome sequencing in elucidating the molecular etiology of congenital limb malformation disorders [15]. Other mutations, unlike polyalanine extension, which tends to form α-helix and causes protein aggregation in the cytoplasm as shown by molecular simulation and immunofluorescence, the c. 925A > T mutation of *HOXD13* impairs downstream transcription of EPHA7 [16]. There is a report speculate that the 11,451 bp microdeletion at chr2:176,933,872–176,945,322 (GRCh37), which is located upstream of *HOXD13* gene (associating with SPD1), which was identified as the smallest deletion upstream of the HOXD13 gene and not altering the sequence of the *HOXD13* gene [17]. We identified a new manifestation of preaxial polydactyly in both hands in a pediatric patient with an expansion of seven alanines, a phenotype not previously noted in SPD patients [18]. Other results showed a 24bp duplication (c.183_206dupAGCGGCGGCTGCGGCGGCGGCGGC

) in the exon 1 of *HOXD13* in heterozygous form which was predicted to result in eight extra alanine (A) residues in N-terminal domain of HOXD13 protein [19].

HOXD13 is the 5' terminal member of the HOXD cluster and has two coding exons. Exon 1 contains an incomplete trinucleotide repeats of GCN (which encodes polyalanine, with N representing A, C, G, or T) and encodes a highly conserved homeobox domain. HOXD13 protein is a transcription factor that must enter the nucleus to regulate downstream target genes [20]. Therefore, the HOXD13 protein may have a nuclear localization signal [21]. Additional amplification of more than seven alanines disrupts this functional region, causing the protein aggregation to form inclusion body in the cytoplasm, thereby preventing the HOXD13 protein from entering the nucleus [22]. These data facilitate the interpretation of synpolydactyly radiographs by future automated tools [23]. In addition, a deep understanding of the key roles of HOXD13 in the most cell types in the bone marrow microenvironment need to explore.

Here, we provided a deep understanding of HOXD13 PAE based on scRNA-sequencing of limb bud samples from synpolydactyly and WT mice. Based on this dataset, we identified osteoclast differentiation related to different cell-type–specific co-expression genes. In line with our results, previous results demonstrated that posterior *HOXD* gene expression similarly stimulated *RUNX2* expression and enhanced the expression of osteoblast-specific osteocalcin (BGLAP), pre-/osteoclast-specific PDGFB, and PTHLH [6]. HOXD13 PAE may alter osteoclast-specific gene expression. Our study is consistent with previous study about the association between osteoclast and SPD in the limb bud of mice [5].

Gene ontology terms of the turquoise module revealed an immune response difference between spdh and WT limbs, which may be supported by a previous study in which knockdown of *HOXD11* or *HOX13* significantly suppressed lung metastasis in immune-deficient mice [6], which is consistent with our results. In addition, our results indicate that *Hoxd13* PAE altered the expression of *Bmp4*, *Hand2*, *Hoxd12*, *Lnp*, *Prrx1*, *Gmnn*, and *Cdc6.* This effect is consistent with recent reports that *Gmnn* is required for *Hox* gene to regulate limb pattern [24]. Many HOX proteins interact with the DNA replication licensing regulator geminin and bind a characterized origin of replication [25]. DNA replication and immune systems are the primary defenses against endogenous and exogenous threats, and defects in these systems are at the core of many health problems, including infections, autoimmune/inflammatory diseases, cancer, and other age-associated diseases. Replication stress can elicit an innate immune response by releasing DNA particles into the cytoplasm. HOXD13 interacts with the *CDC6* loading factor, promotes pre-replication complex protein assembly at origins, and stimulates DNA synthesis in an in vivo replication assay [26]. *Lnp* (Lunapark) was strongly expressed in both limbs and genital buds, and co-expressed with *Hoxd* genes, especially with *Hoxd13* [27]. *Prrx1* and *Hoxd13* were identified as the partner genes, which play important roles in the development of limb [28]. HOXD13 represses the transcription of *SMAD1* and blocks BMP4-SMAD1-induced epithelial mesenchymal transition [29]. In the mouse model of synpolydactyly, polyalanine expansions in Hoxd13 alter the transcriptional program. Our results combine to other's finding, prompt that *HOXD13* involved in the DNA synthesis and regulation of hub genes. PAE is believed to modify DNA replication, which subsequently results in DNA degradation and boost the immune system.

There are two limitations in the present study. First, the generalizability of findings to human synpolydactyly and the specific conditions under which the study was conducted. Second, we did not provide experimental verifying, and further validation of the related mechanism should be done through bench experiments on cell and animal. In this study, we aimed to explore the molecular mechanism using weighted gene co-expression network analysis (WGCNA) of a single-cell RNA sequencing dataset from synpolydactyly limb bud cells. Thus, we mainly focus on the results of bioinformatics analysis.

Conclusions

In summary, WGCNA analysis revealed that synpolydactyly-associated *Hoxd13* PAEs alter the immune response and enhance DNA replication. *Bmp4*, *Hand2*, *Hoxd12*, *Lnp*, *Prrx1*, *Gmnn*, and *Cdc6* were found to play key roles in the development of SPD. Such findings identify possible signaling pathways involved in the pathogenesis of spdh induced by Hoxd13 PAE mutations and advance our understanding of human limb development.

Supplementary Information

The online version contains supplementary material available at https://doi.org/10.1186/s12920-024-01974-9.

Supplementary Material 1.

Supplementary Material 2.

Acknowledgements

We are grateful to Han Wang and Yalin Cheng for their useful comments and suggestions.

Authors' contributions

XC and XZ were responsible for conceptualization, methodology, and software. XS, YC, and TY curated the data and prepared the original draft. XZ revised the manuscript and controlled the decision to publish.

Funding
This work was supported by National Key R&D Program of China (2022YFC2703700) and the grant from the CAMS Innovation Fund for Medical Sciences (2021-I2M-1–051).

Availability of data and materials
All next generation sequencing data generated in the study were deposited at the Gene Expression Omnibus (GEO) under the accession number GSE128818. All data relevant to the study are included in the article or uploaded as supplementary information.

Declarations

Ethics approval and consent to participate
Not applicable.

Competing interests
The authors declare no competing interests.

Received: 4 September 2023 Accepted: 30 July 2024
Published online: 29 October 2024

References

1. Goodman FR. Limb malformations and the human HOX genes. Am J Med Genet. 2002;112(3):256–65.
2. Chintalaphani SR, Pineda SS, Deveson IW, Kumar KR. An update on the neurological short tandem repeat expansion disorders and the emergence of long-read sequencing diagnostics. Acta Neuropathol Commun. 2021;9(1):98.
3. Malik S, Girisha KM, Wajid M, Roy AK, Phadke SR, Haque S, Ahmad W, Koch MC, Grzeschik KH. Synpolydactyly and HOXD13 polyalanine repeat: addition of 2 alanine residues is without clinical consequences. BMC Med Genet. 2007;8:78.
4. Malik S, Grzeschik KH. Synpolydactyly: clinical and molecular advances. Clin Genet. 2008;73(2):113–20.
5. Zhang L, Fang Z, Cheng G, He M, Lin Y. A novel Hoxd13 mutation causes synpolydactyly and promotes osteoclast differentiation by regulating pSmad5/p65/c-Fos/Rank axis. Cell Death Dis. 2023;14(2):145.
6. von Heyking K, Roth L, Ertl M, Schmidt O, Calzada-Wack J, Neff F, Lawlor ER, Burdach S, Richter GH. The posterior HOXD locus: Its contribution to phenotype and malignancy of Ewing sarcoma. Oncotarget. 2016;7(27):41767–80.
7. Basu S, Mackowiak SD, Niskanen H, Knezevic D, Asimi V, Grosswendt S, Geertsema H, Ali S, Jerkovic I, Ewers H, et al. Unblending of Transcriptional Condensates in Human Repeat Expansion Disease. Cell. 2020;181(5):1062–79 e1030.
8. Zhang H, Song L, Wang X, Cheng H, Wang C, Meyer CA, Liu T, Tang M, Aluru S, Yue F, et al. Fast alignment and preprocessing of chromatin profiles with Chromap. Nat Commun. 2021;12(1):6566.
9. Langfelder P, Horvath S. WGCNA: an R package for weighted correlation network analysis. BMC Bioinformatics. 2008;9:559.
10. Storey JD, Tibshirani R. Statistical significance for genomewide studies. Proc Natl Acad Sci U S A. 2003;100(16):9440–5.
11. Wu T, Hu E, Xu S, Chen M, Guo P, Dai Z, Feng T, Zhou L, Tang W, Zhan L, et al. clusterProfiler 4.0: A universal enrichment tool for interpreting omics data. Innovation (Camb). 2021;2(3).
12. Raudvere U, Kolberg L, Kuzmin I, Arak T, Adler P, Peterson H, Vilo J. g:Profiler: a web server for functional enrichment analysis and conversions of gene lists (2019 update). Nucleic Acids Res. 2019;47(W1):W191–8.
13. Szklarczyk D, Franceschini A, Wyder S, Forslund K, Heller D, Huerta-Cepas J, Simonovic M, Roth A, Santos A, Tsafou KP et al: STRING v10: protein-protein interaction networks, integrated over the tree of life. Nucleic Acids Res 2015;43(Database issue):D447–452.
14. Zhao X, Sun M, Zhao J, Leyva JA, Zhu H, Yang W, Zeng X, Ao Y, Liu Q, Liu G, et al. Mutations in HOXD13 underlie syndactyly type V and a novel brachydactyly-syndactyly syndrome. Am J Hum Genet. 2007;80(2):361–71.
15. Melas M, Kautto EA, Franklin SJ, Mori M, McBride KL, Mosher TM, Pfau RB, Hernandez-Gonzalez ME, McGrath SD, Magrini VJ, et al. Long-read whole genome sequencing reveals HOXD13 alterations in synpolydactyly. Hum Mutat. 2022;43(2):189–99.
16. Guo RJ, Fang X, Mao HL, Sun B, Zhou JT, An Y, Wang B. A Novel Missense Variant of Caused Atypical Synpolydactyly by Impairing the Downstream Gene Expression and Literature Review for Genotype-Phenotype Correlations. Front Genet. 2021;12:731278.
17. Jia WM, Zhou XP, Guo NA, Zhang DZ, Hou MQ, Luo YL, Peng XJ, Yang X, Zhang XQ. A novel microdeletion upstream of in a Chinese family with synpolydactyly. Am J Med Genet A. 2022;188(1):31–6.
18. Chen XM, Zhao FY, Xu YM, Cao YX, Li S, Zhang X, Zhao XL. Clinical and genetic analysis in Chinese families with synpolydactyly, and cellular localization of HOXD13 with different length of polyalanine tract. Front Genet. 2023;14:1105046.
19. Zaib T, Ji W, Saleem K, Nie GC, Li C, Cao L, Xu BJ, Dong KX, Yu HF, Hao XG, et al. A heterozygous duplication variant of the gene caused synpolydactyly type 1 with variable expressivity in a Chinese family. BMC Med Genet. 2019;20(1):203.
20. Jung C, Kim RS, Zhang HJ, Lee SJ, Jeng MH. HOXB13 induces growth suppression of prostate cancer cells as a repressor of hormone-activated androgen receptor signaling. Cancer Res. 2004;64(24):9185–92.
21. Williams TM, Williams ME, Heaton JH, Gelehrter TD, Innis JW. Group 13 HOX proteins interact with the MH2 domain of R-Smads and modulate Smad transcriptional activation functions independent of HOX DNA-binding capability. Nucleic Acids Res. 2005;33(14):4475–84.
22. Albrecht A, Mundlos S. The other trinucleotide repeat: polyalanine expansion disorders. Curr Opin Genet Dev. 2005;15(3):285–93.
23. Gottschalk A, Sczakiel HL, Hülsemann W, Schwartzmann S, Abad-Perez AT, Grünhagen J, Ott CE, Spielmann M, Horn D, Mundlos S, et al. HOXD13-associated synpolydactyly: Extending and validating the genotypic and phenotypic spectrum with 38 new and 49 published families. Genet Med. 2023;25(11):100928.
24. Lewis EMA, Sankar S, Tong CL, Patterson ES, Waller LE, Gontarz P, Zhang B, Ornitz DM, Kroll KL. Geminin is required for Hox gene regulation to pattern the developing limb. Dev Biol. 2020;464(1):12–24.
25. Luo LF, Yang XP, Takihara Y, Knoetgen H, Kessel M. The cell-cycle regulator geminin inhibits Hox function through direct and polycomb-mediated interactions. Nature. 2004;427(6976):749–53.
26. Salsi V, Ferrari S, Ferraresi R, Cossarizza A, Grande A, Zappavigna V. HOXD13 Binds DNA Replication origins to promote origin licensing and is inhibited by geminin. Mol Cell Biol. 2009;29(21):5775–88.
27. Francois Spitz FG. Denis duboule: a global control region defines a chromosomal regulatory landscape containing the HoxD cluster. Cell. 2003;113:405–17.
28. Kobzev YN, Martinez-Climent J, Lee S, Chen JJ, Rowley JD. Analysis of translocations that involve the gene in patients with 11p15 chromosomal rearrangement. Gene Chromosome Canc. 2004;41(4):339–52.
29. Fan X, Xun SG, Pan JH, Yue ZY, Shen K, Ji YY, Zhang WW, Zhu YJ, Sha JJ, Wang YQ, et al. HOXD13 suppresses prostate cancer metastasis and BMP4-induced epithelial-mesenchymal transition by inhibiting SMAD1. Int J Cancer. 2021;148(12):3060–70.

Publisher's Note